A 5.5 GHz S_3 Mode Plate Acoustic Wave Resonator Using Lithium Tantalate Thin Film

Zonglin Wu, Shuxian Wu, Hangyu Qian, Feihong Bao*, Guomin Yang , Jie Zou*
Key Laboratory for Information Science of Electromagnetic Waves (MoE), Fudan University
Shanghai, China
baofh@fudan.edu.cn, Jiezou@fudan.edu.cn

Gongbin Tang
New Generation Semiconductor Materials Research Institute, Shandong University
Shandong, China
gongbin.tang@sdu.edu.cn

Acoustic wave resonators using plate acoustic wave in the lithium tantalite ($LiTaO_3$) thin film shows the potential of relating high frequency with a suitable quality factor (Q). The effect of the $LiTaO_3$ thickness on the plate wave characteristics is investigated in this work. A high frequency resonator using third symmetric lamb wave (S_3) mode in a composite plate of 36° *YX*-cut $LiTaO_3$ and silicon dioxide (SiO_2) has been fabricated as a wave-length (λ) is 4 μm. The series resonant frequency (f_s), Q_s and Q_p of the proposed resonator are 5.5 GHz, 419 and 816, respectively. This work demonstrated that the S_3 mode based composite thin film of $LiTaO_3$ and SiO_2 is suitable for high-frequency devices with high Q.

Keywords—plate acoustic wave; high-frequency resonator; quality factor; Lame wave, lithium tantalite.

I. INTRODUCTION

MEMS resonator always shows the potential for some applications in a wide range, such as radio frequency (RF) band-pass filters, sensors, and oscillators [1]-[5]. Along with the increase in communication mobile terminals, the frequencies allocated to wireless communications are difficult to meet existing demand. However, the existing piezoelectric substrates for fundamental acoustic waves cannot meet the requirements of high acoustic velocity in wireless communication, especially if the frequency is higher than 5 GHz. SAW devices shrink the size of MEMS resonators to achieve high frequency with small footprints has resulted in significantly deteriorated Q values. This has led to the emergence of many high-frequency devices that utilize the high acoustic velocity of plate waves [5]-[9] without shirking size. $LiTaO_3$ shows the suitable Q and k^2 approach for high-frequency devices [10]. This work realized a 5.5 GHz composted layers of $LiTaO_3$ and SiO_2 resonator with high-quality factor (Q) by using S_3 Lamb wave mode.

II. SIMULATION AND MEASUREMENT RESULTS

A. Simulation

Plate acoustic waves (PAW)comprise both Lamb wave and shear horizontal wave. Lamb wave has two modes: symmetric (S) and anti-symmetric (A) mode. S_0 and A_0 are fundamental modes, and S_1, S_2, S_3… and A_1, A_2, A_3… are higher modes [2].

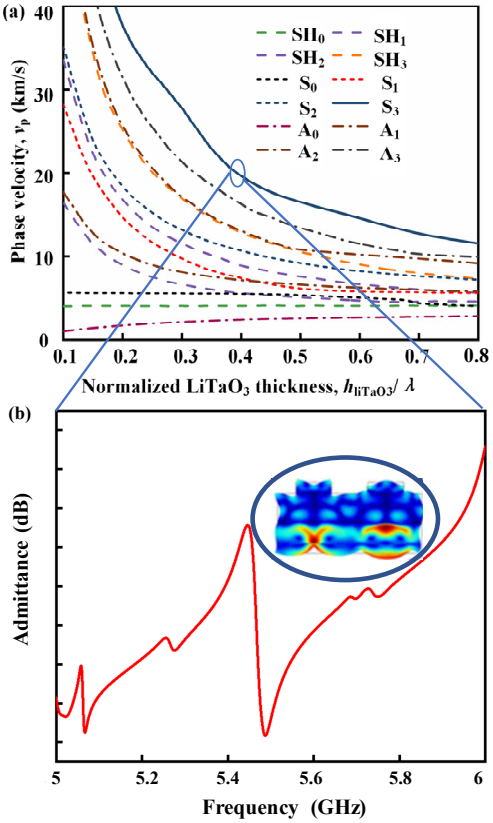

Fig. 1: (a) Simulated phase velocities of the first twelve plate wave mode propagating in LiTaO3 plates as a function of normalized LiTaO3 thickness hLiTaO3/λ, where hLiTaO3/λ takes values from 0.1 to 0.8. (b) Simulated frequency response when h/λ is 0.4 to realize 5.5 GHz resonance frequency.

The effect of different normalized thicknesses (h/λ) on the phase velocities of various modes is investigated by using the FEM simulation software COMSOL. Plate wave modes exhibit a high phase velocity with a strong dispersion, particularly when the ratio h_{LiTaO3}/λ is small. As shown in Figure 1, S_3 mode shows the high velocity where h/λ is from 0.1 to 0.8. Figure 1 shows that when the normalized thickness reaches 0.4, the

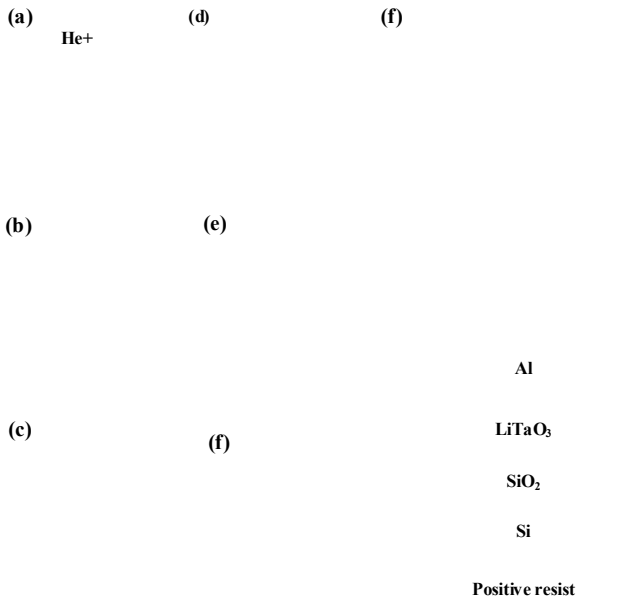

Figure 2: The fabrication flow of the SAW resonators. The fabrication flow can be summarized into seven steps: (a) He^+ implantation into LiTaO3 substrate. (b) Bonding of LiTaO3 substrate to the substrate. (c)Transformation of LiTaO3 substrate into LiTaO3 film by annealing process. (d) Polishing of the LiTaO3 surface. (e) Fabrication of electrodes on LiTaO3 surface using lift-off process. (f) Formation of protective layers using double-sided alignment lithography. (g) Etching with ICP to form an air cavity and removal of photoresist.

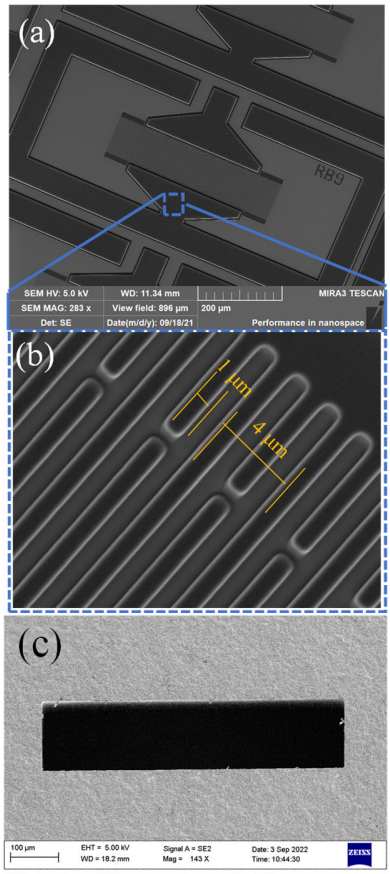

Figure 3: SEM image of the fabricated LiTaO3/SiO2 multilayer plate wave resonator. (a) Top view of the resonator. (b) Zoom-in view of the electrode fingers of the IDT. (c) Bottom view of the fabricated resonator.

phase velocity of S_3 mode is greater than 20 km/s. Therefore, the high phase velocity of S_3 mode is suitable for a 5.5 GHz resonator, as shown in Fig1. (b).

B. Process

The fabrication process is schematically shown in Fig. 2. The process consists of seven steps: (1) He^+ implantation on the surface of the $LiTaO_3$ substrate, (2) bonding of the $LiTaO_3$ substrate to the SiO_2/Si substrate, (3) annealing to convert He^+ into He and splitting the $LiTaO_3$ substrate while retaining the $LiTaO_3$ film on the substrate, (4) polishing the $LiTaO_3$ film surfaces to reduce roughness and repair damaged molecular structure, (5) fabrication of electrodes on the surface through the lift-off process, (6) application of a positive resist to the back of the Si substrate using double-side lithography, and (7) etching of the Si substrate by inductively coupled plasmas (ICP) to form an air cavity.

C. Measurement Result

Fig. 3 displays the top view of a fabricated resonator captured by Scanning Electron Microscope (SEM), with an enlarged view of the IDT as presented in Fig. 3 (a) and Fig. 3(b). From the images, it is evident that the wavelength (λ) is 4 µm, and the width of the electrode finger is 1 µm. Table I provides the geometric dimensions of the fabricated resonator. An SEM image of the backside of the resonator is presented in Fig. 3 (c), showcasing the air cavity range, which includes the region of the IDTs and reflectors that form the $LiTaO_3/SiO_2$ composite plate.

TABLE I. Geometric Dimensions of Resonator.

	$LiTaO_3/SiO_2$ plate
IDT finger number	150
Electrode finger width	1 um
IDT aperture	80 um
Thickness of Al	270 nm
Thickness of $LiTaO_3$ layer	800 nm
Thickness of SiO_2 layer	800 nm

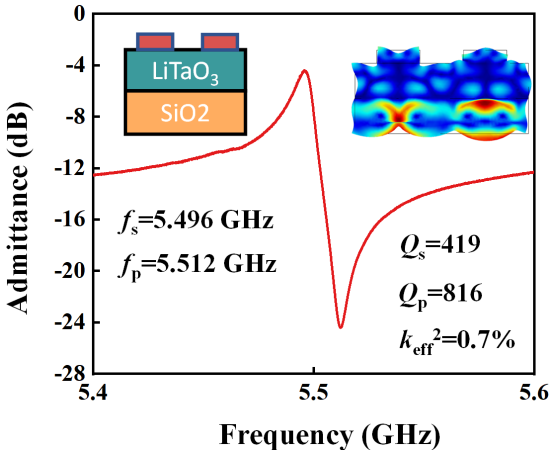

Figure 4: Measured admittance spectra of the S3 mode composited plate wave resonator as wavelength is 4 μm.

The resonator was characterized at room temperature in air using a 150 μm ground-signal-ground (GSG) probe and an Agilent E5071C vector network analyzer. The *Y*-parameters were obtained from the *S*-parameters using a transformation matrix, and the admittance curve was measured and plotted. The resonator exhibited f_s of 5.496 GHz, f_p of 5.512 GHz, and Q_s of 419, and Q_p of 816 when the normalized plate thickness h_p/λ (where h_p is 1.6 μm and λ is 4 μm) of the $LiTaO_3/SiO_2$ composite plate was 0.4, as shown in Fig. 4.

III. Discussion

As shown in Fig. 4, although the resonator realized the 5.5 GHz resonance frequency with high Q, k^2 is small.

According to Berlincourt's formulation [11]:

$$k^2{}_t = \frac{U_{me}}{U_e + U_d} = \frac{\int T : d \cdot EdV}{\int T : s^E : TdV + \int E \cdot \varepsilon^T \cdot EdV} . \quad (1)$$

where U_{me} is the mutual energy, U_e is the elastic energy, and U_d is the electric energy. T is the stress tensor, and E is the electric field. d, s^E and ε^T denote the piezoelectric strain constants, compliance constants at a constant electric field, and permittivity constants at constant stress respectively.

If we want to get a large k^2_t, an U_m needs larger.

$$U_{me} = \int T : d \cdot EdV . \quad (2)$$

Equation (2) signifies the importance of the overlap between the applied lateral electric fields and the stress distribution of the resonant mode inside the piezoelectric material in the thickness direction. The stress distribution of the S_3 mode is not fully overlapped E. It is theoretically possible that A_2 mode could achieve a larger k^2_t. The other reason for S_3 mode shows low k^2 is the piezoelectric constant d is not very consistent with the direction of the electric field. The orientation of the $LiTaO_3$ will change the piezoelectric constant d [12].

IV. Conclusions

In this work, the v_p of the first twelve plate wave modes in $LiTaO_3$ with varying thickness. Plate wave modes exhibit high phase velocity and very strong dispersion, particularly when the h_{LiTaO3}/λ is small. The $LiTaO_3/SiO_2$ composite plate resonator was fabricated by smartcut™ and lift-off and ICP-RIE process. The measured result exhibits f_s of 5.5 GHz, Q_s of 416, and Q_p of 850. These results demonstrate the potential of the S_3 mode in the $LiTaO_3/SiO_2$ composite plate for frequency control, timing reference and sensing applications at high operating frequencies.

References

[1] X. He, K. Chen, L. Kong, and P. Li, "Single-crystalline LiNbO 3 film based wideband SAW devices with spurious-free responses for future RF front-ends," *Appl. Phys. Lett.*, vol. 120, no. 11, p. 113507, Mar. 2022, doi: 10.1063/5.0087735.

[2] S. Kim, M. R. Adib, and K. Lee, "Development of chipless and wireless underground temperature sensor system based on magnetic antennas and SAW sensor," *Sens. Actuators Phys.*, vol. 297, p. 111549, Oct. 2019, doi: 10.1016/j.sna.2019.111549.

[3] Y. Yang *et al.*, "Wireless Multifunctional Surface Acoustic Wave Sensor for Magnetic Field and Temperature Monitoring," *Adv. Mater. Technol.*, vol. 7, no. 3, p. 2100860, Mar. 2022, doi: 10.1002/admt.202100860.

[4] F. Gao, A. Bermak, S. Benchabane, L. Robert, and A. Khelif, "Acoustic radiation-free surface phononic crystal resonator for in-liquid low-noise gravimetric detection," *Microsyst. Nanoeng.*, vol. 7, no. 1, p. 8, Dec. 2021, doi: 10.1038/s41378-020-00236-9.

[5] R. Abdolvand, H. Lavasani, G. Ho, and F. Ayazi, "Thin-film piezoelectric-on-silicon resonators for high-frequency reference oscillator applications," *IEEE Trans. Ultrason. Ferroelectr. Freq. Control*, vol. 55, no. 12, pp. 2596–2606, Dec. 2008, doi: 10.1109/TUFFC.2008.976.

[6] C.-M. Lin, Y.-Y. Chen, V. V. Felmetsger, D. G. Senesky, and A. P. Pisano, "AlN/3C-SiC Composite Plate Enabling High-Frequency and High-Q Micromechanical Resonators," Adv. Mater., vol. 24, no. 20, pp. 2722–2727, May 2012, doi: 10.1002/adma.201104842.

[7] G. Chen and M. Rinaldi, "High-Q X Band Aluminum Nitride Combined Overtone Resonators," in *2019 Joint Conference of the IEEE International Frequency Control Symposium and European Frequency and Time Forum (EFTF/IFC)*, Orlando, FL, USA, Apr. 2019, pp. 1–3. doi: 10.1109/FCS.2019.8856047.

[8] A. Kourani, Y. Yang, and S. Gong, "A *Ku* -Band Oscillator Utilizing Overtone Lithium Niobate RF-MEMS Resonator for 5G," *IEEE Microw. Wireless Compon. Lett.*, vol. 30, no. 7, pp. 681–684, Jul. 2020, doi: 10.1109/LMWC.2020.2996961.

[9] Y. Yang, R. Lu, T. Manzaneque, and S. Gong, "Toward Ka Band Acoustics: Lithium Niobate Asymmetrical Mode Piezoelectric MEMS Resonators," in *2018 IEEE International Frequency Control Symposium (IFCS)*, Olympic Valley, CA, May 2018, pp. 1–5. doi: 10.1109/FCS.2018.8597475.

[10] N. Assila, M. Kadota, and S. Tanaka, "High-Frequency Resonator Using A 1 Lamb Wave Mode in LiTaO 3 Plate," IEEE Trans. Ultrason., Ferroelect., Freq. Contr., vol. 66, no. 9, pp. 1529–1535, Sep. 2019, doi:10.1109/TUFFC.2019.2923579.

[11] K. Hashimoto, Ed., *RF Bulk acoustic wave filters for communications*. in Artech House microwave library. Norwood, Mass. ; London: Artech House, 2009.

[12] W. Yue and J. Yi-jian, "Crystal orientation dependence of piezoelectric properties in LiNbO3 and LiTaO3," *Optical Materials*, vol. 23, no. 1–2, pp. 403–408, Jul. 2003, doi: 10.1016/S0925-3467(02)00328-2.